J. Webster (ed.), *Wiley Encyclopedia of Electrical and Electronics Engineering*

Q-FACTOR MEASUREMENT

This article reports on traditional and modern methods of measurement of the Q-factors of resonators. Many of the techniques which will be described were first developed to determine the Q-factors of microwave resonators. Bearing this in mind, the language of the microwave engineer will be used throughout, although the reader should note that the basic principles are just as applicable to measuring the Q-factors of radio-frequency, millimeter, sub-millimeter, and optical resonators. The chapter will commence with a definition of the Q-factor, and a clear description of the resonator parameters which need to be measured to define the Q-factor of a resonance. The methods of measuring these parameters will then be outlined, including the particular advantages and disadvantages of a technique, the equipment required for the measurement, and the potential for accuracy. Finally, some of the latest developments in the field of Q measurement will be presented.

Measurement of the Q-factor is the measurement of one of the defining characteristics of a resonance. Resonances are seen in devices which are able to store energy for a length of time which is long when compared to the period of oscillation of the electromagnetic energy being stored. The Q-factor is a direct measure of the quality of the resonator, or in other words, the length of time for which the energy can be stored.

To store energy, a resonator must have a method to trap energy. Microwave resonators make use of two main methods to trap energy: storage of the fields in a volume which is surrounded by conductive material, and storage inside a high dielectric material by total internal reflection at the dielectric surface. The first class of resonators are termed microwave cavities, while the second class of resonators are termed dielectric resonators. Of course, it is also possible to build hybrid resonators which use both mechanisms to trap energy. Any electromagnetic field pattern which satisfies Maxwell's equations in the resonator volume and satisfies the boundary conditions imposed by the resonator surfaces is called a normal mode or resonance of the resonator (1).

For energy to enter and leave a resonator, there must be some electrical or magnetic pathway between the resonator and an external transmission line. This pathway is most commonly provided in three ways:

(1) Magnetic loop or electric probe on the end of a coaxial transmission line which protrudes into a cavity resonator,
(2) A direct opening in the metallic wall between a cavity and a waveguide transmission line (iris coupling),
(3) Placing a dielectric resonator in close proximity to a microstrip conductor (evanescent field or reactive coupling).

The number of coupling ports and the type of coupling used on those ports are used to further characterize microwave resonators. Resonators with a single port using probe or iris coupling are termed reflection resonators. Resonators with two or more ports using probe or iris coupling are termed transmission resonators. Two port resonators making use of reactive coupling are termed reactive or absorption resonators.

Microwave resonators, and accurate Q measurements to characterize those resonators, are vitally important in microwave engineering and physics:

(1) Filters can be constructed from resonators because of their selective behavior in the frequency domain. A filter is a device which can transmit or reflect a desired signal while rejecting other nearby unwanted signals.
(2) Measurements of electrical conductivity can be performed by an accurate measurement of the Q-factor of a microwave resonator which has been constructed of the material of interest (2,3). This measurement technique has undergone a renaissance recently with the great interest in high critical temperature superconductors (4).
(3) Microwave properties of materials can be measured by the influences they have on the Q-factor and resonant frequency of a microwave resonance when they are loaded into a microwave resonator (1,5,6). Highly sensitive measurements of the Q and frequency are required to gain accurate material characterization. The dielectric loss and dielectric constants of fluids and gases have been reported by a number of workers using this method (7,8). Magnetic and electrical properties of solids have also been reported (9,10,11,12).
(4) Oscillators which have a high frequency stability in the short term require high-Q resonators; the best stability which has so far been achieved was with a superconducting cavity microwave oscillator operating near 2 K with a Q-factor around 10^{11} (13), and more recently, by a sapphire microwave oscillator at 4 K operating with a Q above 4×10^9 (14).

Microwave Q-factors of interest range from 2 (15) up to 10^{11} for a high perfection superconducting cavity at cryogenic temperatures (13). Coupling factors to these resonances can vary from 10^{-3} for extremely lightly coupled wavemeter resonators up to 10^3 for superconducting cavities at cryogenic temperatures. No single technique can be expected to operate over this full range and always give high resolution and highly accurate measurements. The desire to generate accurate measurements over this full range of interest has led to the large number of Q measurement methods reported here.

Many traditional methods for obtaining the Q factor have fallen from favor either because of improvements in technology, or because the original cumbersome technique can now be circumvented. For example, one of the major reasons for devising time domain Q measuring techniques was to avoid difficulties arising from the typically poor frequency stability of microwave signal generators of the time. However, modern quartz-based synthesizer technology provides a frequency stability which is adequate to measure the Q-factors of all but the very highest Q resonators. A second example is found with the rare use of voltage standing wave ratio ($VSWR$) measurement techniques in modern laboratories. These techniques are slow (16) and cumbersome as they require a device to be moved mechanically to make measurements. Modern network analyzers can make equivalent measurements essentially instantaneously without the need for mechanical changes to the circuit. Nevertheless, traditional Q measurement techniques still have importance because of their simplicity, low cost instrumentation, and instructional value. For these reasons, they will still be discussed below. For highly detailed instructions on performing these methods, the reader should refer to the classical texts (17,18).

Definitions

The letter Q was first used to describe the ratio of reactance to resistance of low frequency inductors and capacitors (18). Because of the usual technique of describing microwave resonators in terms of low frequency circuit elements, the letter Q became associated with describing the ratio of reactance in a resonant circuit to the resistance in that circuit. A simple calculation (see Eq. 3) shows that there is also a close relationship between Q and the time for energy to dissipate in such an equivalent circuit. This led to the incorrect but widespread belief that Q is the initial letter of the expression Q*uality factor* (abbreviated as Q*-factor*), a term related to the length of time that a resonant circuit stores energy. The agreed modern definition of the Q-factor of any general resonant circuit (including electronic, optical, and mechanical resonators) is (18) 2π times the

ratio of energy stored in the system to the energy dissipated per cycle or in symbols,

$$Q = \frac{2\pi U}{\Delta U} \tag{1}$$

where U is the maximum energy of the system, and ΔU is the energy dissipated in a cycle. This equation can be solved to find how the energy decays as a function of time. The energy dissipated in one cycle can be found from

$$\Delta U = -\frac{\partial U}{\partial t}\frac{1}{f_0} \tag{2}$$

where f_0 is the resonant frequency. Substituting Eq. (2) into Eq. (1), the time dependence of U is found as

$$U(t) = U_0 e^{-(\omega_0/Q)t} \tag{3}$$

where U_0 is the initial energy of the resonant system, and $\omega_0 \equiv 2\pi f_0$ is the angular resonant frequency. From inspection of Eq. (3), another more practical definition of Q can be stated: 2 π times the number of cycles required for the energy in the system to decay to $1/e$ of some initial amount or

$$Q = \frac{2\pi\tau}{T_0} \tag{4}$$

where τ is the time taken for the energy to decrease to $1/e$ of its value (called the ring-down time), and $T_0 \equiv 1/f_0$ is the resonant period. As will be seen below, direct use is made of Eq. 4 in determining Q factors by a time domain technique. All other measurement techniques make use of the response of the resonator to forced oscillation. To understand these techniques, we will need to derive expressions which will describe the behavior of the resonator under this condition.

Microwave Resonators. A diagram of a transmission microwave resonator is given in Fig. 1(a). The figure shows an empty metallic cavity where coupling between the resonator and external transmission lines is provided by small openings in the walls of the cavity. A general low frequency analogue to this microwave resonator, its coupling arrangement, and the external transmission lines is given by Fig. 1(b). Each resonance of the cavity is represented by a parallel LCR circuit (19). The kth resonant frequency is given by the expression:

$$(f_0)_k = \frac{1}{2\pi\sqrt{L_k C_k}} \tag{5}$$

and the unloaded Q of the kth resonance can be determined by substituting the energy dissipation provided by R_k and the energy storage provided by C_k and L_k into Eq. 1:

$$(Q_u)_k = R_k\sqrt{\frac{L_k}{C_k}} \tag{6}$$

The iris coupling has been modeled as transformer of unknown turns ratio (17,20). X_{e1} and R_{e1} are the equivalent reactance and shunt resistance of the input coupling network and transmission line, while X_{e2} and

R_{e2} are the equivalent parameters for the resonator output network. R_s is the series impedance of the signal generator, and R_L is the equivalent load resistance of the equipment that is monitoring the resonator. Any measurement of the resonant system represented by Fig. 1(b) will yield a result which is a combination of the properties of the transmission line, the coupling mechanism, and the resonator. However, under certain conditions, it is possible to measure the Q of a particular mode while ignoring the influences of the load, the coupling mechanism, the transmission line, and other modes. In this case, the external impedances can be transformed into the resonant circuit giving the circuit shown in Fig. 1(c). This circuit is far more amenable to analysis and is the model usually assumed by traditional measurement techniques as it greatly simplifies the post-measurement analysis [attempts were sometimes made to allow for coupling losses; i.e., $R_{e1} \neq 0$ (18)]. These simplifications will lead to important errors if the resonator is strongly overcoupled, the Q of the resonance is relatively low, the generator or source are poorly matched to the transmission line, or there is an excessive amount of reactance in the coupling mechanism or transmission line. For the sake of a simple introduction, we will use the circuit shown in Fig. 1(c) and reserve discussion of the more complex situation until the "Modern Measurement Techniques" section later.

To describe how microwave radiation interacts with a resonator, we will use a scattering matrix formalism. Figure 2 shows a voltage wave, $\tilde{a}_1$, incident on an arbitrary microwave two port device. The wave is scattered by the two port, some of its energy going into a reflected wave, $\tilde{a}_2$, and part into a transmitted wave, $\tilde{b}_2$. We express all three waves as

$$A \exp[j(\omega t - \beta z)] \tag{7}$$

where ω is the applied angular microwave frequency, A is the normalized voltage amplitude of the wave, β is the propagation constant, and z is the measurement position. We define the resonator scattering terms s_{11} and s_{21} as

$$s_{11} \equiv \frac{\tilde{a}_2}{\tilde{a}_1} \quad \text{and} \quad s_{21} \equiv \frac{\tilde{b}_2}{\tilde{a}_1} \tag{8}$$

We can, of course, define equivalent parameters for port 2. By substituting Eq. 7 into Eq. 8, we note that s_{11} and s_{21} will depend on the measurement position. This leads to the difficulty that we need to specify the measurement plane each time we quote the resonator scattering parameters. Theoretically, we could avoid this difficulty by always referring the measurement to some special pre-agreed measurement plane, for example, the plane which is coincident with the coupling device. However, practically, it is difficult to make a measurement at that physical position. Instead, we choose to define some special planes which have a well defined measurable characteristic. If a measurement is made of s_{11} at a frequency which is far from the resonant frequency, we can always find a position on the line which responds as if there were a short circuit or an open circuit on the transmission line. These planes are termed the *detuned short* or *detuned open* positions (17,18,20). From the detuned short position, the equivalent low frequency circuit shown in Fig. 1(c) is an accurate representation of the real microwave circuit (given that all the above assumptions still hold). Modern measurements can avoid this difficulty of determining the reference plane (see the Modern measurement techniques section). The scattering parameters at the detuned short position for the circuit shown in Fig. 1(c) have been calculated as (21,22)

$$S_{11}(\epsilon) = \frac{\beta_1 - \beta_2 - 1 - jQ_u\epsilon}{1 + \beta_1 + \beta_2 + jQ_u\epsilon} \tag{9}$$

$$S_{21}(\epsilon) \equiv S_{12}(\epsilon) = \frac{2\sqrt{\beta_1 + \beta_2}}{1 + \beta_1 + \beta_2 + jQ_u\epsilon} \tag{10}$$

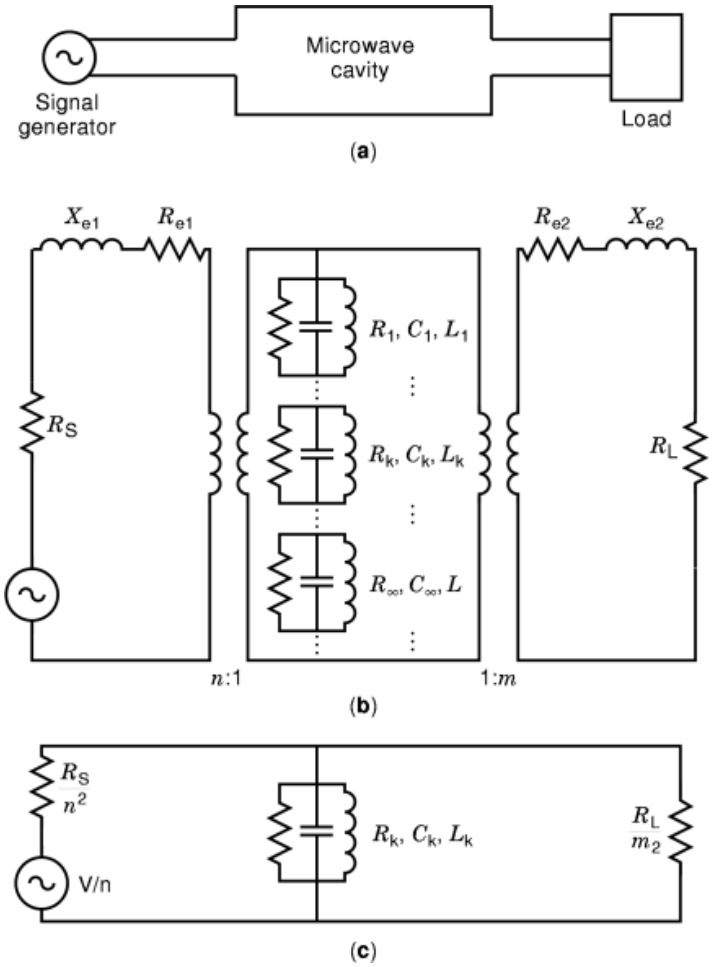

Fig. 1. (a) A diagram of a general microwave cavity resonator with iris coupling on the input and output ports. (b) An equivalent *LCR* circuit for part (a). The cavity resonator has an infinite number of resonances which have been represented by the series of *LCR* circuits: $(R_1, C_1, L_1), \ldots, (R_k, C_k, L_k), \ldots, (R_\infty, C_\infty, L_\infty)$. The input and output coupling network have been modeled with a series loss (R_{e1}, R_{e2}) and series inductance (X_{e1}, X_{e2}) to take into account any losses or reactance of the coupling network. The source and load series impedance are denoted by R_s and R_L. The iris coupling has modeled as a transformer of unknown turns ratio. (c) A highly simplified version of part (b), where the traditional assumptions of Q-factor measurement have been made. The coupling reactance and loss are assumed to be zero. The source and load are assumed to have a resistance which is perfectly matched to the line impedance. All other resonances of the cavity are assumed to be sufficiently far from the resonance of interest that they can be safely ignored. All external components have been transformed across the transformers and into the resonant circuit.

where $\varepsilon \equiv f/f_0 - f_0/f$, f is the incident frequency, f_0 is the resonant frequency as defined above in Eq. 5, Q_u is the unloaded Q of the resonator as defined in Eq. 6, and the coupling factors are defined as the ratio of the internal resonant resistance to the external resistances when transformed into the resonant circuit; that is,

$$\beta_1 = \frac{n^2 R_k}{R_s} \quad \text{and} \quad \beta_2 = \frac{m^2 R_k}{R_L} \tag{11}$$

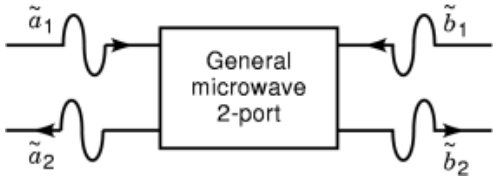

Fig. 2. Schematic diagram representing the scattering of microwave voltage waves by a microwave two-port.

where n is the effective turns ratio of the input coupling mechanism, and m is the effective turns ratio of the output coupling mechanism. If $\beta < 1$, then a resonator is termed undercoupled; if $\beta > 1$, then a resonator is termed overcoupled; and if $\beta = 1$, then the resonator is critically coupled. Eq. 9 also applies to single port reflection resonators if β_2 is set to zero.

It is useful to split Eqs. 9 and 10 into their real and imaginary parts as this will give us the in-phase response and quadrature phase response of the resonator, respectively. In other words, the real part of Eq. 9 gives us the portion of the reflected wave which is in phase with the incident signal and the imaginary part will give the fraction of the reflected signal, which is $\pi/2$ out of phase with the incident signal.

$$\text{Real}[s_{11}] = \frac{(1+\beta_1+\beta_2)(\beta_1-\beta_2-1)-\epsilon^2 Q_u^2}{(1+\beta_1+\beta_2)^2+\epsilon^2 Q_u^2} \tag{12}$$

$$\text{Imag}[s_{11}] = \frac{-2\beta_1\epsilon Q_u}{(1+\beta_1+\beta_2)^2+\epsilon^2 Q_u^2} \tag{13}$$

$$\text{Real}[s_{21}] = \frac{2\sqrt{\beta_1\beta_2}(1+\beta_1+\beta_2)}{(1+\beta_1+\beta_2)^2+\epsilon^2 Q_u^2} \tag{14}$$

$$\text{Imag}[s_{21}] = \frac{-2\sqrt{\beta_1\beta_2}\epsilon Q_u}{(1+\beta_1+\beta_2)^2+\epsilon^2 Q_u^2} \tag{15}$$

An interesting and novel way of summarizing this information is by using a three dimensional parametric plot of the resonator response as a function of frequency (see Fig. 3 for a plot of s_{11}). If we make two dimensional projections of this plot along the principal axes, we will see response curves that are more familiar to the microwave engineer. To display this, we have projected the three dimensional plot onto the faces of the box in Fig. 3 and then rotated these faces into view. Viewing the curve which has been projected onto the plane perpendicular to the real axis we see the imaginary response of the resonator [Fig. 3(b)], looking along the imaginary axis, we observe the real response of the resonator [Fig. 3(c)], and finally, looking parallel to the frequency axis, we observe a circle—which is termed the Q circle of the resonator [Fig. 3(d)]. This horizontal projection plane is more readily recognized as the Smith Chart (23). The Smith Chart gives the magnitude of s_{11} by the distance that a plotted point is from the origin, while the phase of s_{11} (ϕ) is given by the angle that the line joining the point to the origin makes with the real axis. The most important advantage of this three dimensional description of the resonator response is the clear demonstration of the intimate relationship which exists between the many descriptions of microwave resonators given in the literature: the real and imaginary components of the scattering matrix, the Smith Chart, and the magnitude and phase of the response.

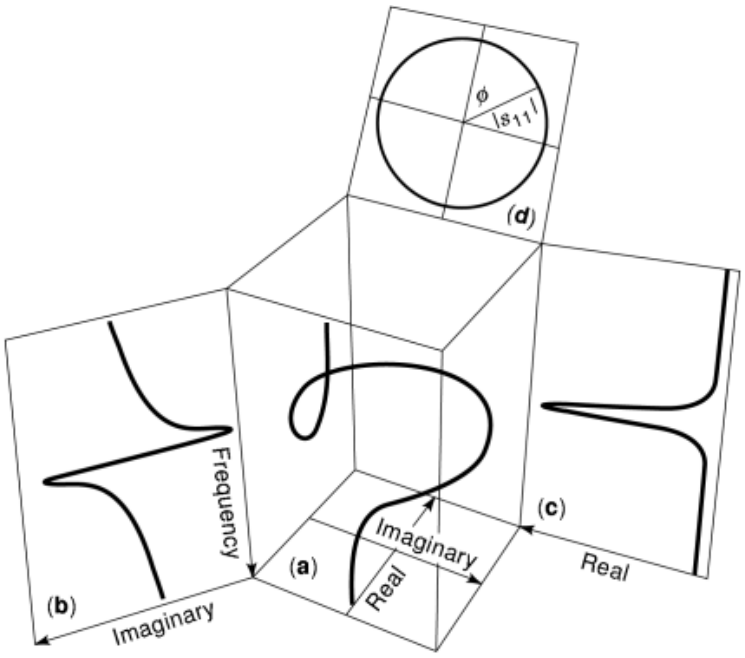

Fig. 3. (a) A three dimensional display of the scattering parameter, s_{11}, from a reflection resonator. The curve has been projected onto the faces of the box, and then these faces have been rotated into view. (b) Shows the imaginary (or quadrature phase) reflection response of the resonator. (c) Shows the real (or in-phase) reflection response of the resonator. (d) Shows the Q-circle of the resonator on a Smith Chart. The phase and magnitude of the reflection coefficient at a particular frequency are given by the distance that a plotted point is from the origin and the angle it makes with the real axis.

Q-factor measurements of two port microwave resonators frequently employ measurements of the transmitted and reflected power as a function of frequency. In cases of moderate to high Q, the derived frequency variable ε can be simplified with negligible error to

$$\epsilon = \frac{2\Delta f}{f_0} \tag{16}$$

where $\Delta f \equiv f - f_0$. We will term Δf the frequency detuning. The squared magnitude of s_{11} and s_{21} (which gives the reflected and transmitted power coefficients respectively) can be derived from Eqs. 9 and 10 as

$$|s_{11}|^2 = \frac{(1-\beta_1+\beta^2)^2 + 4\left(\frac{Q_u \Delta f}{f_0}\right)^2}{(1+\beta_1+\beta_2)^2 + 4\left(\frac{Q_u \Delta f}{f_0}\right)^2} \tag{17}$$

$$|s_{21}|^2 = \frac{4\beta_1\beta_2}{(1+\beta_1+\beta_2)^2 + 4\left(\frac{Q_u \Delta f}{f_0}\right)^2} \tag{18}$$

Plots of these functions have been given on Fig. 4.

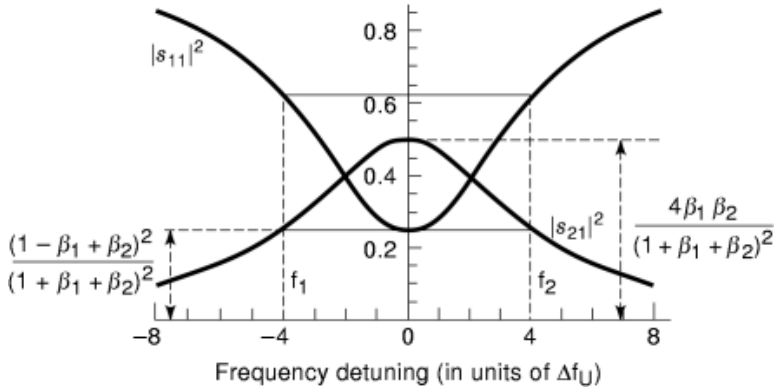

Fig. 4. The power reflection and transmission coefficients of a two port resonator with $\beta_1 = 1$ and $\beta_2 = 2$. The loaded Q of the resonator is given by $Q_L = f_0/(f_2 - f_1)$, where f_1 and f_2 are the points at which the power transmission coefficient is half the maximum power transmission, or the points where the power reflection coefficient is the average of the on and off-resonance power reflection coefficients.

Loaded Q (Q_L), Unloaded Q (Q_U) and External Q (Q_e). There are three distinct Q-factors of which we commonly talk when we discuss the losses in a microwave circuit. The unloaded Q (Q_U) is the Q-factor that would be measured as the electromagnetic coupling to the resonator tended to zero. That is, it is associated with dissipation which occurs inside the resonator (R_k in Fig. 1(c) and see Eq. 6). The external Q (Q_e) is the dissipation which occurs external to the resonator but which is coupled into the resonance by the coupling to the external circuit [R_s and R_L in Fig. 1(c)]. We can derive an expression for the external Q-factors in the same way as we found the unloaded Q factor (Eq. 6):

$$Q_{e1} = \frac{R_s}{n^2}\sqrt{\frac{C}{L}} \quad \text{and} \quad Q_{e2} = \frac{R_L}{m^2}\sqrt{\frac{C}{L}} \tag{19}$$

The loaded Q (Q_L) is the Q-factor measured by any scalar Q measurement method. It includes the contributions of all losses in the circuit which provide a dissipation mechanism for the resonance (both internal and external to the resonant circuit). We can write the relationship between the loaded Q, the unloaded Q, and the external Q factors as

$$\frac{1}{Q_L} = \frac{1}{Q_U} + \frac{1}{Q_{e1}} + \frac{1}{Q_{e2}} \tag{20}$$

Using the definitions of the coupling factors (Eq. 11) and the definitions of the unloaded and external Q factors (Eqs. 6 and 19), we can simplify Eq. 20 to

$$Q_u = (1 + \beta_1 + \beta_2)Q_L \tag{21}$$

General Q-Factor Measurement Techniques. Let us simplify some of our original expressions to generate some practical ways to measure the Q factor. From an examination of Eq. 17, we see that the maximum power transmitted through the resonator occurs when the incident frequency is exactly equal to the resonant frequency. As we move away from the resonant frequency, the transmitted power falls as the square of the frequency difference. An important measure of such a resonant curve would be its sharpness. We choose to

measure the sharpness of the curve by the frequency difference between the two frequency values which transmit half the maximum power; that is, we need to find the frequency detuning Δf which satisfies the equation:

$$|s_{21}(\Delta f)|^2 = \frac{1}{2}|s_{21}(0)|^2 \tag{22}$$

The solution to Eq. 22 is

$$\Delta f = \pm\frac{1}{2}\frac{(1+\beta_1+\beta_2)f_0}{Q_{\mathrm{U}}} = \pm\frac{1}{2}\frac{f_0}{Q_{\mathrm{L}}} \tag{23}$$

Let us define a new parameter, Δf_{L}: the loaded half bandwidth which is equal to the positive solution of Eq. 23; that is,

$$\Delta f_{\mathrm{L}} = \frac{1}{2}\frac{f_0}{Q_{\mathrm{L}}} \tag{24}$$

Equation 23 gives us a method of measuring Q_{L} in transmission resonators. By measuring the resonant frequency, the maximum transmission power and the two frequency points at which the transmitted power is down by half, we can calculate the loaded Q.

To derive Q_{u} from this measurement, we will need to determine the coupling factors and use Eq. 21. By measuring the reflected power coefficient on resonance and the transmitted power coefficient on resonance, we have two equations with two unknowns (Eqs. 17 and 18). These can be solved to find the coupling coefficients:

$$\beta_1 = \frac{(\Gamma_0 \pm 1)^2}{1-\Gamma_0^2-T_0^2} \quad \text{and} \quad \beta_2 = \frac{T_0^2}{1-\Gamma_0^2-T_0^2} \tag{25}$$

where $\Gamma_0 = |s_{11}(0)|$ and $T_0 = |s_{21}(0)|$. The first of these two equations can also be applied to finding the coupling coefficient for a one port resonator by letting β_2 be equal to zero. The equation can then be rewritten as

$$\beta_1 = \frac{1 \pm \Gamma_0}{1 \mp \Gamma_0} \tag{26}$$

It is not possible to determine which of the two solutions in Eq. (25) or (26) is, in fact, the correct one if we are limited to a scalar power transmission method of determining the Q-factor. We need to measure some phase information (16), or vary the physical coupling in a known way (18,24), to remove this ambiguity. If one is not interested in knowing the coupling factors individually but just for the purpose of determining the unloaded Q factor from the loaded Q factor, then one can use (22)

$$1+\beta_1+\beta_2 = \frac{2}{s_{11}(0)+s_{22}(0)} \tag{27}$$

If it is possible to measure the complex components of s_{11} either directly, with a network analyzer or using a phase bridge, or indirectly, through measurements of the line VSWR, then there are some alternative methods

to estimating the Q-factor of a resonator. For simplicity, we will perform the following calculations for a one port reflection resonator ($\beta_2 = 0$). However, it should be noted that the equations which govern reflection, transmission, and reaction resonators are all essentially equivalent (25), and so, most Q measurement techniques can be applied to all three types of resonator (25,26).

We need to determine the relationship which exists between the real and imaginary components of s_{11} when at a particular frequency detuning. This relationship may then be used to measure the Q. Let us define an unloaded half bandwidth in the same way as we did for a loaded half bandwidth (Eq. 24):

$$\Delta f_{\mathrm{U}} \equiv \frac{1}{2}\frac{f_0}{Q_{\mathrm{U}}} \tag{28}$$

Substituting Δf_L and Δf_U into the real and imaginary parts of s_{11} (Eqs. 12 and 13), we find the following relationships:

$$\mathrm{Im}[s_{11}(\pm\Delta f_{\mathrm{L}})] = \mp\{1 + \mathrm{Re}[s_{11}(\pm\Delta f_{\mathrm{L}})]\} \tag{29}$$

$$\mathrm{Im}[s_{11}(\pm\Delta f_{\mathrm{U}})] = \mp\left\{1 - \sqrt{2 - (\mathrm{Re}[s_{11}(\pm\Delta f_{\mathrm{U}})])^2}\right\} \tag{30}$$

If the frequency detuning is varied until one of the above equations are satisfied, the value of the detuning will be equal to the loaded or unloaded half bandwidth. By back substitution into Eqs. 28 and 24, the unloaded and loaded Q may be found.

General Sources of Errors in *Q* Measurement

We can divide measurement error into two categories: systematic and random. Systematic error yields a consistent result on repeated measurements of a constant resonance but with a value which differs from the true value. Such a measurement would be termed one with high resolution but relatively poor accuracy. Random errors (noise) will result in a scattering of results on repeated measurements of a constant resonance. If the measurement system is dominated by random noise, it is relatively easy to estimate its accuracy by just making multiple measurements of a constant resonance and quoting some statistical measure of the deviation. An improvement in the quality of the measurement can also usually be made by averaging multiple measurements. An estimation of the accuracy of a system which is dominated by systematic errors is far more difficult. Typically, one would try to use two or more completely independent measurement techniques to measure the same resonance and quote the differences between the results.

Systematic *Q* Measurement Errors. Any Q estimation technique which samples the scattering parameters at a number of different frequencies requires that we place conditions on the amplitude and frequency stability of the source to achieve a given accuracy. Any constant drift in the source frequency during the measurement will result in distortions to the resonance curve shape with a consequent distortion of the loaded Q value. Drifts in the amplitude of the source will give rise to distortions in the measured coupling factors which will give errors in the estimation of the unloaded Q. The relative error in the Q-factor under these conditions depends on the order in which the measurements are taken. However, for a worst case estimate, if we assume the measurements are taken in ascending or descending frequency order and are equally spaced, then we can

estimate the fractional error in estimation of Q_L as

$$\frac{\Delta Q_L}{Q_L} = \pm \frac{tkQ_L}{f_0} \tag{31}$$

where t is the time required to sample the response between $+\Delta f_L$ and $-\Delta f_L$, and k is the frequency drift rate of the source in Hz/s.

Drifts in the resonant frequency of the resonance during the measurement will also cause distortions to the measured Q values in much the same way as drifts in the source frequency. This is especially important when the temperature coefficient of the resonator is large, and the resonator Q-factor is high. For example, in the case of a sapphire dielectric resonator at 77 K, the fractional frequency temperature coefficient is around 10^{-5}/K, while Q_L is around 5×10^7 (27). Temperature drifts of the order of 200 μK during the period of measurement will limit the accuracy of the Q-factor measurement to 10%.

Almost all frequency domain Q-measurements have traditionally relied on being able to treat the resonance as a single resonance which is well described by an equivalent LCR network. In the situation where there are losses or reactance in the coupling network, or there are interfering resonances in the resonator or in the external transmission lines, there will be distortions to the classic resonance shape with consequent errors in the measured Q factors. It is difficult to give a summary of the errors induced by ignoring these effects as there are so many possibilities. However, for example, the Q circles method (see below) will give a Q_U which is 15% in error for each 1 dB of return loss which is ignored in the lines leading to a critically coupled resonator.

In resonators which are remote from the experimental apparatus, or in systems with poorly matched loads and sources, resonances can appear in the connecting transmission lines which cause distortions to the resonance shape. The best solution to this problem is to suppress these spurious resonances by using microwave isolators to better match the load and source. To overcome large amounts of coupling reactance or interfering resonances in the resonator, itself, one must refer to some of the methods covered in the "Modern measurement techniques" section below.

If the resonator contains materials which have properties (either reactive or resistive) which are altered by the amplitude of the incident microwave fields, there is a strong possibility the resonator will exhibit a level of nonlinear behavior (28,29). For example, resonators which have been loaded with maser materials such as ruby can exhibit Q-factors which are negative under certain conditions (28). If high power microwave sources are being used, it is also possible for temperature changes to be induced in the resonator which cause resonant frequency changes, or for electrical breakdown to occur. Most superconducting cavities demonstrate a very strong Q dependence on power (3). Under all these circumstances, great care must be taken to ensure that correct results are obtained. For example, the Q-factor can be measured at a number of different incident powers to determine if a consistent result is being obtained.

Finally, any errors in the calibrations of the measuring instruments will lead to inaccuracies in the measurement. For example, Sucher (18) has calculated the error in measurement of the Q of a transmission resonator from an error in the attenuation measurement (ΔA) of the half power transmission points to be

$$\frac{\Delta Q_L}{Q_L} = -0.23 \Delta A \tag{32}$$

Thus, a 0.1 dB error in measurement leads to an inaccuracy of 2.3%.

Random *Q* Measurement Errors. Random noise in parts of the measurement apparatus will lead to random variations in the measured Q value of an unchanging resonance. Many of the mechanisms mentioned in the previous section are also applicable to this section if, rather than smooth drift of the variable, it exhibits noisy behavior. For instance, rapidly varying frequency noise (phase noise) of the microwave source will create

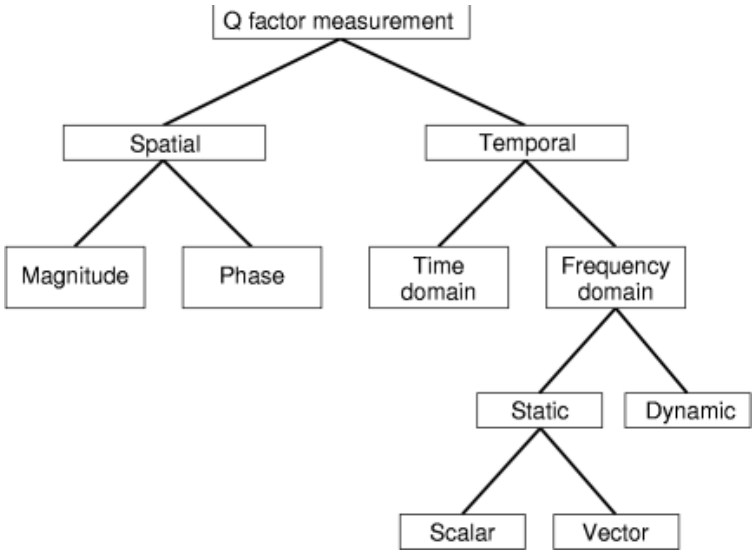

Fig. 5. The Q factor measurement techniques described in this chapter have been divided into the classification scheme which is shown in this figure.

an amplitude noise in the reflected or transmitted power. This will limit the experimenter's ability to identify a particular point on a resonance curve. For example, to measure a typical X-band dielectric resonator Q of 10^5 to an accuracy of 1% requires that the position of the measured frequency points is determined to better than 1 kHz. Such frequency stability is only achieved by modern quartz synthesized microwave signal sources.

All Q measurements will be ultimately limited by the intrinsic noise of the amplitude or phase sensor in the analyzing instruments. The fractional noise in the Q measurement is given approximately by the fractional noise in the power measurement. It is very rare that this ultimate limit is achieved in practice as the other noise sources (particularly the frequency noise in the source) conspire to increase the measurement noise level.

Traditional Methods of *Q* Measurement

The methods of Q measurement have been classified into the categories shown in Fig. 5. A major distinction has been made between spatial and temporal techniques because of the very different technology required for the two types of measurement. Spatial techniques rely on using a slotted line device to measure the voltage standing wave ratio ($VSWR$) in the incident microwave line. The VSWR gives a measure of the magnitude of the reflection coefficient of the resonator, and the positions of the voltage minima in the VSWR pattern give a measure of the reflection phase.

Temporal measures of the Q include measurements made in both the frequency and time domains. Frequency domain measures are the most commonly used techniques today. These techniques rely on measuring either or both of the components of the scattering parameters as a function of frequency. This can be done in a step-wise measurement of the scattering parameter at a number of frequency points, or it can be done with a continuously swept source as long as the time of the sweep is much longer than the ring-down time of the resonance. The term *static* in Fig. 5 implies that measurements are made slowly compared to the ring-down time, and that the measured output signal is synchronous with the source frequency sweep. Dynamic measurements are also made with a sweep which is slow compared to the ring-down time of the resonance,

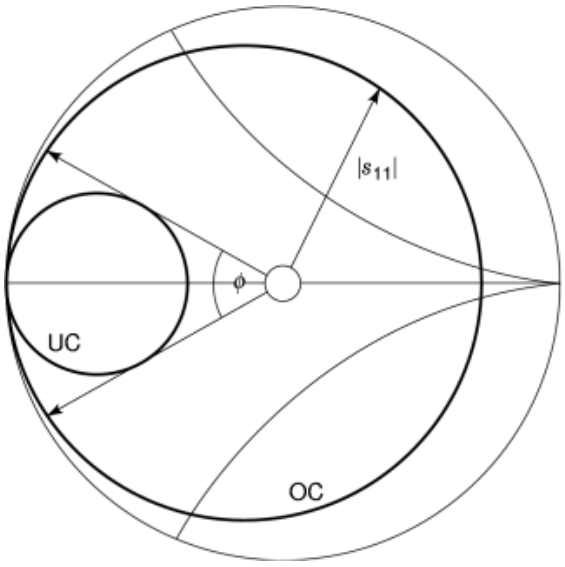

Fig. 6. Smith Chart plots of the s_{11} responses of over (OC) and undercoupled (UC) resonances. The reflection phase of the OC resonance changes by 2π across the resonance, while the reflection phase of the UC resonance reaches a maximum value of $\phi/2$ before returning to zero and then reaching a minimum value of $-\phi/2$ before once again returning to zero. The relative changes in magnitude of the reflection coefficient are much larger in the case of the undercoupled resonator.

but in these measurements, the output signal is at a harmonic of sweep rate, and so they are intrinsically AC measurements.

Spatial Methods: Phase and Amplitude. If a measurement were made of the voltage along the incident line of the microwave resonator in Fig. 2, we would find a standing wave formed by the interference of the incoming and outgoing waves. The ratio of the minimum to maximum voltage as measured along this transmission line is termed the VSWR and can be directly measured with a slotted line device. The locations of the voltage minima (or maxima) in this pattern are determined by the phase of the reflected signal. The amplitude of the VSWR is given by

$$\text{VSWR} = \frac{1 + |s_{11}|}{1 - |s_{11}|} \tag{33}$$

To compare s_{11} for under and overcoupled resonators, a plot of each is given on a Smith Chart in Fig. 6 (as viewed from the detuned short position). One notes that $|s_{11}|$ (and hence the VSWR also) of an overcoupled resonator is large and relatively constant although the reflection phase changes by $2\ \pi$ across the resonance. The undercoupled resonance demonstrates a relatively small phase variation although the relative VSWR change is large. This knowledge arms the engineer for an accurate measurement of the Q using a slotted line device. If the resonator is overcoupled, then a measurement of the position of the voltage minima should be made, while if the resonator is undercoupled, then a measurement of the magnitude of the VSWR will yield the more accurate result.

Substitution of Eq. 9 into Eq. 33 yields the result that the VSWR on resonance is equal to $\beta^{\pm 1}{}_1$ for a one port resonator. A measurement of the VSWR alone is unable to resolve the sign of the exponent although an additional quick measurement can determine this (see below).

The VSWR at $\pm\Delta f_{\mathrm{L}}$ and $\pm\Delta f_{\mathrm{U}}$ for the undercoupled case can be calculated as a function of the VSWR on resonance (V_0) to be

$$\mathrm{VSWR}(\pm\Delta f_{\mathrm{L}}) = \frac{\left|\dfrac{j+V_0}{1+V_0}\right| + 1}{\left|\dfrac{j+V_0}{1+V_0}\right| - 1} \quad \text{and}$$
$$\mathrm{VSWR}(\pm\Delta f_{\mathrm{U}}) = \frac{\left|\dfrac{1-(1+j)V_0}{1+(1+j)V_0}\right| + 1}{\left|\dfrac{1-(1+j)V_0}{1+(1+j)V_0}\right| - 1} \tag{34}$$

Thus, if we measure V_0, substitute it into the equation above, and then measure the frequency detuning at which the VSWR is equal to the calculated value, we can immediately determine Q_{U} and Q_{L}.

For overcoupled resonators, the Q is accurately determined by measuring the position of the voltage minima (or maxima) as the resonant frequency is changed (for a tunable resonator) or as the incident signal frequency is changed. A plot of the position of the voltage minima for two one-port resonators ($\beta_1 = 0.6$ and 1.6) is given in Fig. 7 as a function of resonant frequency. The relatively large change in the position of the minima for overcoupled resonators is clearly visible. The points on the overcoupled resonator curve which are most easily identified experimentally occur where the minima shift is $\pm\pi/2$ (this is half the maximum shift). Given that the phase shift on reflection from the resonator is given by

$$\phi = \mathrm{ArcTan}\left[\frac{\mathrm{Im}[s_{11}]}{\mathrm{Re}[s_{11}]}\right] \tag{35}$$

we see that a phase shift of $\pm\pi/2$ occurs when the real part of s_{11} (Eq. 12) is equal to zero. Solve this to find the $\pi/2$ frequency detuning points:

$$\Delta f_{\pi/2} = \pm\frac{1}{2}\frac{f_0}{Q_{\mathrm{U}}}\sqrt{\beta_1^2 - 1} \tag{36}$$

So a measurement of the frequency detuning which gives a $\pi/2$ shift combined with a measurement of the VSWR when the resonator is tuned to resonance will yield the unloaded Q of the resonator.

Figure 7 also suggests a simple method to determine whether a resonator is under or overcoupled. For undercoupled resonators, we note that the position of the minima is the same when the resonator is tuned exactly to resonance and when it is tuned far from resonance. This is not the case for overcoupled resonators. Thus if the slotted line probe is adjusted onto a voltage minimum at resonance, and then the resonant frequency is shifted so that it is far from resonance, only in the case of an undercoupled resonator will the probe still be at a voltage minimum.

Time Domain Techniques.

Decrement Method. The decrement method is one of the older methods of measuring the Q factors of high Q resonators (17,18). Before the advent of quartz based microwave synthesizers, the frequency stability of the best Gunn oscillators and klystrons meant that measurements of Q factors higher than 10^{4--5} would be

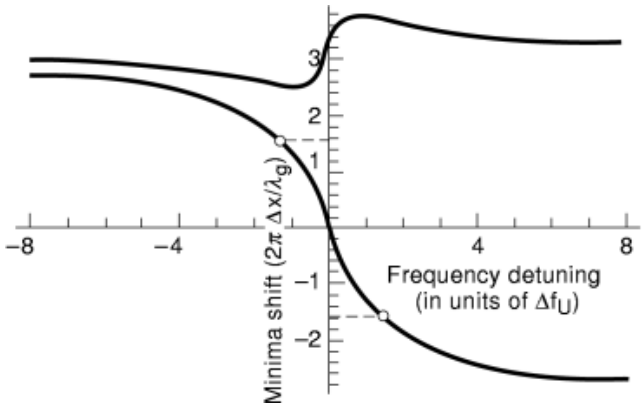

Fig. 7. Calculated position shift (in radians) of the minima in the VSWR pattern as a function of resonant frequency for two resonances with $\beta_1 = 0.6$ (upper curve) and 1.6 (lower curve). The position shift is seen to be much larger for the overcoupled resonator which is in accordance with our prediction from the Smith Chart plot in Fig. 6.

inaccurate. To overcome this difficulty, a method to excite the resonance and measure the time for the energy to dissipate was developed.

A microwave oscillator which can have its output power switched on or off by an external signal is driven by a pulse generator with a repetition rate much slower than the resonator ring-down time (Eq. 4). This pulsed generator also triggers an oscilloscope which is monitoring the energy leaking from the resonator from either the input or output port using a crystal detector. The power leaking from the resonator is proportional to the stored energy in the resonator. If the crystal detector has an accurate square law response, that is, its output voltage is proportional to the incident power, then the oscilloscope screen display is an accurate representation of Eq. 3, and the Q is directly determined by measuring the time taken for the signal to drop by a factor of e. This time interval can then be substituted into Eq. 4 and the loaded Q determined.

Care must be taken to ensure that the microwave source frequency remains resonant and that the source output power is constant; otherwise, the oscilloscope trace moves vertically causing difficulty with an accurate measurement of the time interval. To avoid this difficulty, a method making use of a continuously swept source has been suggested (30). The source is swept across the resonance, and when it becomes resonant, an electronic circuit monitoring the transmitted power automatically switches the source off and triggers the oscilloscope. Using modern equipment, decrement techniques can easily measure loaded Q-factors near 10 GHz in the range upwards from 10^{4--5} (ring down times longer than a few microseconds).

Inaccuracies enter the decrement techniques if the bandwidth of the power detector and/or the oscilloscope is inadequate to correctly capture the transient response of the resonator. The measured Q factor will also be in error if the crystal detector does not give an output which is strictly proportional to input microwave power.

Unfortunately, all time domain methods give no information on the coupling and, hence, can only measure the loaded Q of the resonators. This difficulty may be overcome if it is possible to vary the coupling to the resonator. In this case, the coupling can be made progressively smaller until the measured Q does not change with any further reduction in coupling. At this point, the measured loaded Q will be equal to the unloaded Q to within the experimental resolution. The accuracy of the decrement techniques is directly proportional to the fractional error in the estimation of the ring-down time.

Fast Sweep Decrement Method. The fast sweep decrement method (31) is a modification of the decrement method with three advantages: the researcher can make use of more widely available CW sweep microwave generators rather than the pulsed generator required above, the required frequency stability of the microwave source is much less stringent, and no sophisticated electronics are required.

This measurement is suitable for a reflection resonator and requires a microwave detector to monitor the signal reflected from the resonator. The source is swept over a frequency range which is much wider than the bandwidth of the resonance with a sweep repetition rate (seconds per sweep cycle) which is much longer than the ring-down time of the resonator. The frequency sweep rate (Hz/s), however, is set such that the source sweeps across the resonance in a time which is much shorter than the ring-down time. An instant after the sweep has passed through the resonance, the detector mounted on the reflected port receives two signals: the reflected off-resonance signal which has a frequency corresponding to the frequency of the source at this instant, as well as the weak signal leaking from the resonator at the resonant frequency. The detector mixes these two signals giving rise to a characteristic frequency chirp (caused by the frequency difference having a time dependence) which has an exponential envelope following the decreasing strength of the leaking signal. From (31), we see that the envelope of the chirp has an exponential time constant which is twice as long as that seen in the normal decrement method; that is,

$$Q_L = \pi \tau_e f_0 \tag{37}$$

where τ_e is the time required for the signal envelope to decrease to $1/e$ of its amplitude. A measurement of τ_e yields Q_L.

A colleague (32) has developed an automatic Q measuring system which can provide relatively high resolution results based on this technique. By monitoring the dc and ac voltage output from the reflected power detector, one can calculate the incident power on the resonator as well as a value which is proportional to the amplitude of the chirp. The amplitude of the chirp is proportional to both the incident power and the Q of the resonance. By forming the ratio of the ac and dc voltage, one can calculate a number which is proportional to the loaded Q factor of the resonance. The constant of proportionality can be determined by an initial calibration using one of the other techniques for measuring Q. From then on, a new value for the loaded Q is generated after every sweep cycle. The technique gives measurements with a resolution of around 5% under typical conditions. The technique has proved very useful when the Q is changing quickly as a function of time.

Scalar Static Frequency Domain Techniques.

Half-Power Points Technique. We have already outlined a method to determine the loaded Q from a transmission measurement where we determined the frequency point at which half the on-resonance power is transmitted and then directly substituted into Eq. 23 to calculate Q_L. However, an implicit assumption is made in Eq. 23 that one can identify the resonant frequency accurately to calculate the value of Δf. However, because the resonance shape is flat at the center of resonance, it is frequently difficult to identify this point accurately. Furthermore, the fractional error induced in the Q is extremely sensitive to an error in the calculation of Δf arising from a misidentification of the resonant frequency (Δf_0):

$$\frac{\Delta Q_L}{Q_L} = \frac{\Delta f_0}{f_0} Q_L \tag{38}$$

Since we can measure source frequency differences very accurately using an electronic frequency counter, a better method of measuring the Q relies on measuring the two frequencies f_1 and f_2 at which the transmission power is down by half from the on-resonance value (17,18):

$$f_1 - f_0 = \frac{1}{2}\frac{f_0}{Q_L} \quad \text{and} \quad f_2 - f_0 = \frac{1}{2}\frac{f_0}{Q_L} \tag{39}$$

If we form the difference of these two equations, we get

$$f_1 - f_2 = \frac{f_0}{Q_L} \tag{40}$$

where we can determine Q_L without the need for an accurate determination of f_0 (see Fig. 4). An additional measurement of the on resonance reflection and transmission coefficients (Eq. 25) gives us the coupling information needed to calculate Q_U.

Nonetheless, it is important to note that for an accurate measurement of the Q using this method, the requirements on the attenuation measurement are extremely stringent (Eq. 32). An alternative microwave bridge method has been proposed which can find the half transmission points very accurately (33).

Calibrated Attenuator Method. One of the difficulties of the Half-Power points technique is the necessity for an accurately calibrated power detector. To avoid this difficulty, we can make use of a calibrated attenuator. This method relies on finding the maximum transmission point, while there is a 50% attenuator placed in the signal path between the microwave source and the detector. This attenuation is then removed, and the source detuned to the two frequency points at which the original output voltage is regained on the detector. Once again, the loaded Q is calculated using Eq. 40.

Reflected Power Technique. To determine the power reflected from a one port resonator at $\pm\Delta f_L$, we substitute into Eq. 17 to get

$$|s_{11}(\pm\Delta f_L)|^2 = \frac{1+\beta_1^2}{(1+\beta_1)^2} \tag{41}$$

Thus, to measure the loaded Q, we need to measure the reflection coefficient on resonance and calculate the coupling using Eq. 26. We then substitute this into Eq. 41 and calculate the power reflection coefficient at the loaded half-bandwidth frequency points. Finally, we measure the frequency detuning corresponding to this power reflection in the resonator, and from this frequency detuning, we can calculate Q_L and Q_U.

Straight-Line Methods. Another method for measuring the Q factor from the scalar reflection or transmission coefficients has been suggested where transformed frequency coordinates are used so that the resonance shape appears to be linear (18,34,35). This method lends itself to either a manual graphical solution or a simple least squares fit on a computer. We can rearrange Eq. 17 for a one port resonator [we can also do the same thing for the transmission coefficients (34)] to define a new variable:

$$\delta_U(\Delta f) \equiv \left(\frac{Q_U \Delta f}{f_0}\right) = \pm\sqrt{\frac{(1+\beta_1)^2|s_{11}(\Delta f)|^2 - (1-\beta_1)^2}{1-|s_{11}(\Delta f)|^2}} \tag{42}$$

If we have calculated β_1 from a measurement of the on-resonance reflection coefficient (see Eq. 25), then for each measurement of s_{11} we can calculate a value for the variable δ_U (all values are known on the right hand side of Eq. 42). If we make a plot of these values of δ_U as a function of frequency detuning (Δf), we will find a straight line which has a slope equal to Q_U/f_0. From the slope, we can clearly generate the unloaded Q (35).

When implemented in a computer based system, this technique has the potential for excellent high accuracy measurements of the order of 0.01% for Q-factors of the order of 10^4 (34). This accuracy arises because the measurement makes use of reflection data which is in close proximity to the center of resonance and because of the enormous amount of data which can be taken. By limiting the data to that near the center of resonance, there is a reduction in the effect of interference from other resonator and transmission lines

modes. To achieve the accuracy reported, the researchers used nearly 1000 data points to characterize the resonance. This technique also has another advantage in that the degree of linearity of the plot is a measure of the level of interference from other modes. This immediately gives the experimenter an idea of the veracity of the measurement.

A similar method to the above mentioned one has been suggested in connection with transmission measurements at 93 GHz (36,37). One of the potential problems with the above method is finding the exact center of resonance. Any errors in this identification introduce a large error because Δf in Eq. 42 will be incorrect (see Eq. 38). If we define a new variable, m,

$$m^2 \equiv \frac{|s_{21}(0)|^2}{|s_{21}(\Delta f)|^2} \tag{43}$$

then we can rewrite Eq. 18 as

$$m^2 = 1 + 4\left(\frac{Q_L \Delta f}{f_0}\right)^2 \tag{44}$$

If we measure the left hand side of Eq. 43 at a known frequency detuning, we can immediately calculate Q_L from Eq. 44. However, any error in the measurement of the resonant frequency will introduce large errors. We would like to perform the calculation in a way which is insensitive to the exact value of the resonant frequency. If we make a measurement of m^2 at two frequency points on either side of the resonance, we can rewrite Eq. 44 as

$$\begin{aligned} \Delta f_1 = f_1 - f_0 &= \frac{-f_0}{2Q_L}\sqrt{m_1^2 - 1} \quad \text{and} \\ \Delta f_2 = f_2 - f_0 &= \frac{f_0}{2Q_L}\sqrt{m_2^2 - 1} \end{aligned} \tag{45}$$

If we take the difference of these two equations, we can derive a further equation to define Q which is only dependent on a frequency difference which, in principle, we can measure very accurately:

$$Q_L(f_1, f_2) = \frac{f_0}{2(f_1 - f_2)}\left(\sqrt{m_1^2 - 1} + \sqrt{m_2^2 - 1}\right) \tag{46}$$

If we make N measurements of m^2 on either side of the resonant frequency, then we have N^2 pairs of m values. From each pair, we can calculate a value for Q_L using Eq. 46. The variance of the ensemble of Q_L values is a measure of the closeness with which the data follows the theoretical resonance curve. If there is any systematic variation of Q_L as a function of frequency, it suggests the effects of interfering resonances. This method, is therefore, a very useful indicator of the isolation of the resonance (38).

Single Frequency Technique. As mentioned above, resonators and the resonator Q factor are commonly used to measure the electrical, optical, or magnetic properties of materials. These measurements are usually undertaken by measuring the properties of a resonator before and after making some change to that resonator such as, for example, inserting a small sample into the resonator, changing the illumination level on a sample already in the resonator, or changing the resonator temperature. In these cases, we are more interested in a measurement of the change in Q rather than an absolute measurement of the Q-factor. The single frequency

measurement technique determines changes in the Q-factor essentially instantaneously and doesn't require measurements in the time or frequency domain (39,40).

If the change we have made to the resonator is such that the electromagnetic field distribution near the coupling ports is unchanged, then we can expect that the coupling ratios m and n in Fig. 1 will remain unchanged. If the change causes a modification to the losses in the resonator (R_k in Eqs. 6 and 11), then both the unloaded Q and coupling will change, but the ratio of these two parameters will remain constant:

$$\frac{Q_u}{\beta_1} = \frac{R_s}{n^2}\sqrt{\frac{L_k}{C_k}} = C \tag{47}$$

where C is some constant. Thus, if we continuously monitor the reflected power at resonance, we can determine any changes in the coupling, and from Eq. 47, the fractional change in Q_U will be exactly equal to the fractional change in coupling.

Dual Resonator Techniques. A novel method for determining all resonator parameters from a simultaneous measurement of two resonators has been described by a number of authors (41,42,43). In these techniques, the power transmission and/or reflection coefficient of a resonator is plotted as a function of the transmission coefficient of a tunable reference cavity. The output plots are a function of the difference in resonant frequency of the two resonators and the ratio of their Q factors. Analytic expressions for the shapes of these curves have been derived in terms of the difference frequency and Q factor ratio, and these can be adjusted to fit experimentally derived measurements (41,43). The accuracy of this method is similar to those of the other techniques reported here ($\sim$2%), although it is necessary to know the Q factor of the reference cavity in advance of these measurements using one of the other methods. The big advantage of the technique is that it is unnecessary to use calibrated power detectors, although the detectors must have a matched response. The second major advantage arises because the data is represented on a parametric plot so any source frequency instability is suppressed. The quality of the measurement is determined by the stability of the reference cavity.

Integration Technique. If a frequency stable source and/or calibrated power measuring device is unavailable so that accurate measurements of the half power transmission points are impossible then an integration method can be used (44). If we integrate the transmitted power coefficient (Eq. 18) as a function of frequency, we obtain the following expression:

$$\int_{-\infty}^{\infty} |s_{21}|^2 d\Delta f = \frac{P_0 \pi f_0}{2Q_L} \tag{48}$$

where P_0 is the power transmitted at the resonant frequency. This equation can be implemented experimentally if we use a microwave sweep oscillator to sweep the frequency over many loaded bandwidths and use an analog integrator to integrate the output of a crystal detector on the transmission port of the resonator. An additional measurement of the output voltage of the detector when the generator is on-resonance determines the only other unknown parameter so that Q_L can be determined.

The integration method has also been proposed as an accurate method to determine the small changes in Q associated with determining losses in materials via resonator perturbation methods (45).

Numerical Methods. One of the earliest computer-based methods of measuring the Q factor was reported by Pandrangi et al. (46). A computer directed a Voltage controlled Oscillator (*VCO*) to step through the resonance curve of a transmission resonator at around 1 GHz. The incident and transmitted power were monitored by detectors which were, in turn, monitored by the computer. The power transmission coefficient was obtained by a division of these signals and a polynomial fitted to a smoothed version of this data. By differentiation of this polynomial, the inflection points of the resonance curve were found (see Fig. 8). To find how the inflection

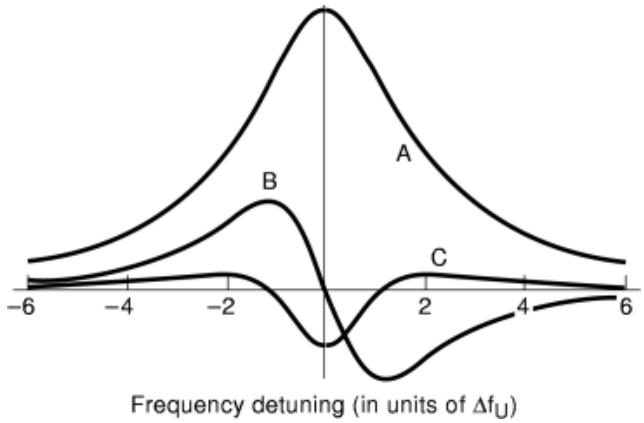

Fig. 8. A plot of the frequency dependence of the power transmission coefficient (A), as well as its first (B) and second derivative (C), with respect to frequency (arbitrary vertical scale). Note that the curve possesses two inflection points (points where the second derivative is equal to zero).

points are related to the Q, we need to find when the second frequency derivative of Eq. 18 is equal to zero; that is,

$$\frac{\partial^2}{\partial \Delta f^2}\{|s_{21}(\Delta f_{\text{inf}})|^2\} = 0 \tag{49}$$

which has as its solution

$$\Delta f_{\text{inf}} = \pm \frac{f_0}{2\sqrt{3}Q_{\text{L}}} \tag{50}$$

The experimental results were limited by frequency instability in the VCO to around 5%.

Frequency Lock Technique. An interesting method for accurately measuring the phase as a function of frequency is presented in the paper by Linzer et al. (47). In this method, a Klystron is frequency locked to a resonator. Typically, any frequency locking system is set up to detect the imaginary part of the reflection or transmission coefficient and then use this to stabilize the oscillator. If a phase offset is introduced into the feedback mechanism so that the locking system is now partially sensitive to the real part of the reflection coefficient as well, then it will lock at some distance from the center of resonance. The particular dependence of the oscillator frequency on this phase shift is determined by the loaded Q of the resonator, and hence by a measurement of the frequency offset in the system as a function of the feedback phase shift, the loaded Q can be measured with an accuracy of around 1–2%.

Vector Static Frequency Domain Methods.

Q Circles Method. If one measures both the phase and magnitude (or real and imaginary components) of s_{11} using either the VSWR method, a reflection bridge (48), or a network analyzer, then it is possible to plot s_{11} directly on a Smith Chart. If plots of the loci of Eqs. 29 and 30 for all Δf_{L} and Δf_{U} are also placed on the chart, then the intersections of the s_{11} curve and these two solution sets give the loaded and unloaded half bandwidths. This graphical solution method is outlined in detail by Ginzton (17).

Straight-Line Methods. If one can measure the real and imaginary components of s_{11} or s_{21} of a resonator separately, then one can plot the following ratios as a function of Δf for each of the different resonator types:

$$\frac{\mathrm{Im}[s_{11}(\Delta f)]}{\mathrm{Re}[s_{11}(\Delta f)]}[\text{reaction Eq. (49)}],$$
$$\frac{\mathrm{Im}[s_{21}(\Delta f)]}{\mathrm{Re}[s_{21}(\Delta f)]}(\text{transmission}),$$
$$\frac{\mathrm{Im}[s_{11}(\Delta f)]}{\mathrm{Re}[s_{11}(\Delta f)]+1}(\text{reflection})$$

All of these ratios yield a straight line with a slope of $2Q_{\mathrm{L}}/f_0$. Clearly by a measurement of the slope of these straight line plots, we can measure Q_{L}.

Dynamic Frequency Domain Techniques. There are two main dynamic frequency domain techniques, the harmonic or inflection point technique and the intermodulation method. Both of these techniques rely on the fact that at two frequency points on either side of the resonant frequency, there are points where the second derivative of the resonance curve is equal to zero (see Fig. 8 and Numerical Methods above). It is important to note that the sweep rates (Hz s^{-1}) for both of these techniques need to be much slower than $(f_0/Q_{\mathrm{L}})^2$ for the measurement to be accurate. In this sense, the measurements are still quasi-static, although we have chosen to term them dynamic because the measurement is made at a frequency which differs from the sweep frequency.

Harmonic (Inflection Points) Technique. If a frequency modulated signal is incident on the resonance curve shown in Fig. 8, and we monitor the power of the transmitted signal, it is clear that part of the frequency modulation (*FM*) will be converted to amplitude modulation (*AM*) by the resonator. If the frequency deviation is small, the amplitude of the transmitted AM at the fundamental FM frequency will be proportional to the slope of the curve measured at the carrier frequency. If the resonance has nonzero curvature; that is, if the second derivative is not zero, then the transmitted signal will also contain an AM component at the second harmonic of the FM. Thus, a measurement of the amplitude of the second harmonic AM as a function of frequency will yield a curve which is proportional to that shown as the second derivative curve (C) on Fig. 8. Since extremely sensitive synchronous detection techniques exist (such as lock in amplifiers), this method can very accurately find the points for which there is no second harmonic AM (17,18). Using Eq. 50 this value can be easily converted to the loaded Q of the resonator.

Intermodulation Method. A potential problem arises in the previous method if the FM signal is not completely free from higher harmonic content. If the incident signal already contains the second harmonic component, then the measurement of the inflection points will be in error. To avoid this, we can make use of an intermodulation method. If we simultaneously frequency modulate an incident signal at two different frequencies, then it is clear that we will generate AM components in the transmitted signal at the two fundamental FM frequencies. However, if there is any non-linearity of the curve, then we will also generate AM components at the difference and sum frequency of the two components. If we set our system to detect one of these intermodulation components, such as the difference frequency, then we can be sure that this could only have been generated via the nonlinearity of the resonance curve (17,18). Once again, when identification of the inflection points is completed, we can calculate Q_{L} using Eq. 50.

Modern Measurement Techniques

Because of the advent of powerful personal computers for data analysis, combined with the wide availability of microwave equipment with computer interfaces, many new techniques have been devised recently which

allow the lifting of the restrictions which were previously placed on Q measurement. For example, accurate measurements can now be made in the presence of a transmission line or coupling reactance. An additional advantage of computer aided measurement is that large numbers of measurements, which would be tedious to take manually, are easily made. The data averaging which occurs from using such large numbers of data samples gives improved immunity to random noise in the Q measurement. This section will describe some of these latest methods and is divided into sections which highlight the major advantage of the technique.

Scalar High Resolution Measurements. Luiten et al. (50) have developed a new data averaging technique which doesn't require the use of expensive network analyzers and relies on measurement of the square of the magnitude of the reflection or transmission coefficient as a function of frequency. The acquired data is then fitted using a nonlinear algorithm to the expected shape of a completely general resonance (Eqs. 17 or 18). The fitting mechanism is adaptive, which gives the program a robustness and an ability to follow resonances if the resonance parameters change smoothly with time. This feature was used to great advantage to measure the temperature dependence of thermal, electrical, and magnetic properties of TiO_2 and Al_2O_3 crystals (10). The extreme frequency stability of the source in this case (fractional frequency stability $\sim 10^{-15}$) meant that the Q measurements had a resolution of 0.03% despite the loaded bandwidth being only 10 Hz.

Kajfez (24) has developed a technique which uses a scalar network analyzer to measure the values of the reflection coefficient as a function of frequency. This technique takes into account moderate coupling losses and, therefore, allows the off-resonance reflection coefficient to differ from 1. When compared to vector curve-fitting methods, this technique, like all scalar techniques, suffers from the disadvantage that it is impossible to tell whether a resonator is over or under-coupled. Nonetheless, its accuracy appears to be comparable to the vector methods ($\sim$0.2%).

Vector High Resolution Measurements. A simple modification to the Q-circles method has been suggested by Hearn et al. (51) to take into account losses in the coupling network. It can be shown that Eq. 30 is equivalent to the condition that the magnitude of the real and imaginary parts of the impedance of the resonator are equal. In the case where there is loss in the coupling mechanism or the transmission lines, a correction needs to be made; otherwise, the estimated Q will be less than the true value. Hearn et al. (51) have suggested a simple correction which reduces the errors of the traditional measurement by around 80 times in the case of high coupling loss and small coupling. Unfortunately, this correction cannot be implemented with a simple Smith Chart overlay, although it is easily implemented in a automated measurement system.

Sanchez et al. (49) report an absorption resonator Q measurement system based on a computer driven network analyzer. This system empirically removes the effects of any loss in the coupling network, or transmission lines, by rescaling the data by a factor obtained from the transmission coefficient far from resonance. A fit is performed to the Q-circle from which the coupling and Q is found. The Q_U measurement error is around 1%.

Kajfez (52,53) has developed a method which uses a network analyzer combined with a computer analysis to generate and fit Q-circles [Figs. 3(d) and 6]. Instead of graphically finding the solutions, he uses a least square fitting routine to an expression which includes the effects of frequency independent line and coupling reactance as well as any losses in the coupling network. This technique avoids the ambiguity that exists between over and under-coupled resonators in scalar techniques. The technique's accuracy is estimated as around 0.1% when utilizing approximately 1000 data points.

In the presence of significant line inductance, we find that instead of the ideal circle which should be seen in a plot of the real and imaginary components of the resonator impedance, we find a curve which is nearly circular but with a smaller diameter and which crosses over itself (54). By finding the two frequencies corresponding to the crossing over point as well as those corresponding to the maximum and minimum of the imaginary impedance component (the critical points), we can determine Q_U very accurately. These measurements are relatively easy using a modern network analyzer and will generate Q-factors which have an accuracy of about 0.5%.

Measuring Resonance Parameters in Presence of Other Resonances. Kajfez et al. (55) have developed an overlay for a network analyzer which takes into account the effects of inductance and loss in the coupling and transmission network as well as the effects of any distant resonant modes. These effects are modeled as a frequency dependent reactance in a series with the mode of interest. The effect of this frequency dependent series inductance is to cause the Q circle to develop distortions which make its apparent diameter smaller than it would otherwise be. If an accurate determination of the reference plane of the measurement is made, this technique can also measure the inductance of the coupling network.

Sauer et al. (56) have modeled the effects of reflections which exist in the lines between the measuring apparatus and the resonator under test. These reflections create subsidiary line resonances which distort the resonance shape and create errors in the measurement of the Q-factor. The model can accurately fit experimental data taken in the presence of interfering line resonances yielding a Q-factor with an accuracy of $\sim$1%.

An extensive analysis and experimental procedure has been developed which allows for the accurate measurement of Q factors and coupling coefficients of two or more modes which are in extremely close proximity (19,57). The process relies on developing an expression which fully represents the circuit shown in Fig. 1(b) with enough free parameters to represent all visible resonance curves in the data as well as an additional frequency dependent term to represent any coupling reactance. The free parameters are then adjusted by a least squares fitting procedure to the experimental data. Even in the situation where a double loop is visible on the Smith Chart because two resonances are within a few bandwidths of each other, the accuracy of the Q measurement is around 2%.

Measuring Extremely Low Resonators. Resonators measurements are generally made through transmission lines or coupling networks which have poorly understood characteristics. The interaction of these external networks causes distortions to the resonance and, therefore, to the apparent Q-factor. This is an especially difficult problem when the Q factor of the resonator is low as the frequency rate of change of the resonator impedance becomes comparable to that of the external circuit parameters. Kajfez et al. (58) have developed an expression for determining Q_{U} when it is measured through an arbitrary two port. Using a similar approach, Drozd et al. (15) have developed a general Q-factor measuring method based on the full s_{11} parameters as determined by a computer driven network analyzer. The loaded Q is shown to be given by

$$Q_{\mathrm{L}} = \frac{\omega_0}{2R_{\mathrm{k}}}\left|\frac{dX_{\mathrm{k}}}{d\omega}\right| \tag{51}$$

where X_{k} is the total reactance of the kth resonance and R_{k} is the total resistance of the kth resonance. The frequency derivative of the reactance is estimated from a number of measurements of s_{11} in the immediate neighborhood of center frequency of the resonance. Measuring near to the center of resonance gives immunity from the influences of stray inductance in the transmission line and coupling mechanism. This method proves to be far more accurate than a measurement of the half-power points or of the critical points, both of which are relatively distant from the resonant frequency. In addition, this method does not make the common assumption of Eq. 16 which is really only valid when the Q is greater than a few thousand. As a result, this method yields accurate results even for Q-factors of the order of 2.

Oscillator Phase Noise Determination. Fuchs (59) has made use of Leeson's (60) relation that in a simple microwave oscillator, the loaded Q-factor of the resonator directly determines the phase noise of the oscillator. By artificially introducing high levels of component phase noise, the oscillator noise floor becomes dominant over the phase noise measurement system's internal noise. From a plot of the phase noise of the oscillator, the loaded Q can be directly determined to an accuracy of around 10%.

Theoretical *Q* Estimates. Theoretical estimation of Q factors has always been extremely difficult for all but the simplest metallic cavities with known surface resistance. Recently, a number of attempts have been

made to model more complex hybrid dielectric resonators and estimate the Q factors on purely theoretical grounds (38,61,62). These estimates have value in that they could allow an independent verification of the veracity of Q measurement techniques. Unfortunately, as the accuracy of these calculations is still only around 10%, their predictive power is not yet useful in determining the accuracy of various measurement techniques.

Acknowledgement

The author would like to thank Tony Mann for a critical reading of the manuscript. He would also like to thank all the personnel of the Sapphire Clock and Low Phase Noise Oscillator projects at UWA for providing an innovative and challenging environment in which to work.

BIBLIOGRAPHY

1. H. B. G. Casimir On the theory of electromagnetic waves in resonant cavities, *Philips Res. Rep.*, **6**: 162–182, 1951.
2. D. Kajfez A. Gundavajhala Measurement of material properties with a tunable resonant cavity, *Elec. Lett.*, **29** (22): 1936–1937, 1993.
3. C. M. Lyneis *Experimental Studies of Microwave Properties of 8.6GHz Superconducting Niobium, Niobium-Tantalum, and Tantalum Cavities*, Ph.D. Thesis, Department of Physics, Stanford University, California, 1974, unpublished.
4. J. Ceremuga J. Krupka T. Kosciuk Resonant measurements of surface resistance of high-T_c superconducting films: How good or bad are they?, *J. Superconductivity*, **8** (6): 681–689, 1995.
5. J. J. Hinds W. H. Hartwig Materials-properties analyzers using superconducting resonators, *J. Appl. Phys.*, **42** (1): 170–179, 1971.
6. M. N. Afsar J. R. Birch R. N. Clark The measurement of the properties of materials, *Proc. IEEE*, **74**: 183–199, 1986.
7. G. Birnbaum J. Franeau Measurement of the dielectric constant and loss of solids and liquids by a cavity perturbation technique, *J. Appl. Phys.*, **20**: 817–818, 1949.
8. G. Johri R. Ngoui J. Roberts A study of experimental and theoretical shifts in a resonant microwave cavity loaded with polar and non-polar molecules in the gas phase, *J. Microw. Power Electromagn. Energy*, **24** (4): 227–235, 1989.
9. D. Grissom William H. Hartwig Dielectric dissipation in NaCl and KCl below 4.2K, *J. Appl. Phys.*, **37** (13): 4784–4789, 1966.
10. A. N. Luiten A. G. Mann D. G. Blair Paramagnetic susceptibility and permittivity measurements at microwave frequencies in cryogenic sapphire resonators, *J. Phys. D: Appl. Phys.*, **29**: 2082–2090, 1996 and A. N. Luiten et al., Microwave properties of a Rutile resonator between 2–10K, *Meas. Sci. Tech.*, 1998, in press.
11. N. Klein *et al.* Dielectric properties of rutile and its use in high temperature superconducting resonators, *J. Appl. Phys.*, **78** (11): 6683–6686, 1995.
12. R. J. Deri Dielectric measurements with helical resonators, *Rev. Sci. Instrum.*, **57** (1): 82–86, 1986.
13. S. R. Stein J. P. Turneaure Superconducting cavity stabilized oscillators with improved stability, *Proc. IEEE*, 63: 1249–1250, 1975.
14. A. N. Luiten *et al.* Latest results of the UWA cryogenic sapphire oscillator, *Proc. 49th Freq. Control Symp.* (FCS), San Francisco, 433–437, 1995.
15. J. M. Drozd W. T. Joines Determining Q Using S Parameter Data, *IEEE Trans. Microw. Theory Tech.*, **MTT-44**: 1996.
16. J. R. Ashley F. M. Palka Reflection Coefficient Measurement of Microwave Resonator Q Factors, *Microw. J.*, **14**: 35–39, 1971.
17. E. L. Ginzton *Microw. Meas.*, New York: McGraw-Hill, 1957.
18. M. Sucher Measurement of Q, in volume **II** *Handbook of Microwave Measurements*, M. Sucher and J. Fox, (eds.) New York: Wiley, 417–493, 1963.
19. W. P. Wheless D. Kajfez Experimental Characterization of Multimoded Microwave Resonators Using Automated Network Analyzer, *IEEE Trans. Microw. Theory Tech.*, **MTT-35**: 1987.
20. K. Kurokawa *An Introduction to the Theory of Microwave Circuits*, New York: Academic Press, 1969.

21. Z. Galani *et al.* Analysis and Design of a single resonator GaAs FET oscillator with Noise Degeneration, *IEEE Microw. Theory Tech.*, **MTT-32**: 1556–1565, 1984.
22. D. H. Han Y. S. Kim M. Kwon Two Port cavity Q measurement using scattering parameters, *Rev. Sci. Instrum.*, **67** (6): 2179–2181, 1996.
23. P. H. Smith *Electronic Applications of the Smith Chart in Waveguide, Circuit and Component Analysis*, New York: McGraw-Hill, 1969.
24. D. Kajfez Q-factor measurement with a scalar network analyzer, *IEE Proc.—Microw. Antennas Propag.*, **142** (5): 369–372, 1995.
25. M. C. Sanchez E. Martin J. M. Zamarro Unified and simplified treatment of techniques for characterizing transmission, reflection or absorption resonators, *IEE Proc.*, **137** (4): 209–212, 1990.
26. A. Khanna Y. Garault Determination of Loaded, Unloaded and External Quality Factors of a Dielectric Resonator Coupled to a Microstrip Line, *IEEE Trans. Microw. Theory Tech.*, **MTT-31**: 261–264, 1983.
27. M. E. Tobar *et al.* Low Noise Microwave Oscillators Based On High-Q Temperature Stabilized Resonators, *Proc. 48th IEEE Int. Freq. Control Symp.*, 433–440, 1994.
28. A. E. Siegman *Microwave Solid State Masers*, New York: McGraw-Hill, 1964.
29. J. Petykiewicz Chapter 10.14, *Wave Optics*, Dordrecht: Kluwer Academic, 1992.
30. A. Kocherzhin *et al.* Device for Measurement of High Q values by Attenuation, *Instrum. Exp. Tech.*, **31** (2): 494–496, 1988.
31. H. J. Schmitt H. Zimmer Fast Sweep Measurements of Relaxation Times in Superconducting Cavities, *IEEE Trans. Microw. Theory Tech.*, **MTT-14**: 206–207, 1966.
32. A. G. Mann Physics Department, University of Western Australia, unpublished communication.
33. K. Watanabe I. Takao A bridge method for simultaneous measurements of coupling coefficient and loaded Q of a single ended cavity, *Rev. Sci Instrum.*, **44** (11): 1625–1627, 1973.
34. K. D. McKinstry C. E. Patton Methods for determination of microwave cavity quality factors from equivalent circuit models, *Rev. Sci. Instrum.*, **60** (3): 439–443, 1989.
35. Z. Frait C. E. Patton Simple Analytic method for microwave cavity Q determination, *Rev. Sci. Instrum.*, **51** (8): 1092–1094, 1980.
36. R. K. Mongia R. K. Arora Accurate measurement of the Q factor of an open resonator in the W frequency band range, *Rev. Sci. Instrum.*, **63**: 3877–3880, 1992.
37. R. K. Arora S. Aditya X. Xu Computer Aided Measurement of Q-factor with Application to Quasi-Optical Resonators, *IEEE Trans. Instrum. Meas.*, **IM-40**: 863–866, 1991.
38. R. K. Mongia *et al.* Accurate Measurement of Q-factors of Isolated Dielectric Resonators, *IEEE Trans. Microw. Theory Tech.*, **MTT-42**: 1463–1467, 1994.
39. V. Subramanian J. Sobhanadri New Approach to measuring the Q-factor of a microwave cavity using the cavity perturbation technique, *Rev. Sci. Instrum.*, **65** (2): 453–455, 1994.
40. B. Tian W. R. Tinga Single-Frequency Relative Q Measurements Using Perturbation Theory, *IEEE Trans. Microw. Theory Tech.*, **MTT-41**: 1922–1927, 1993.
41. G. Magerl K. R. Richter A Novel Method for Cavity Parameter Measurement, *IEEE Trans. Instrum. Meas.*, **IM-25**: 145–151, 1976.
42. G. Magerl Fast Measurement of Cavity Coupling Coefficients, *IEEE Trans. Microw. Theory Tech.*, **MTT-26**: 223–224, 1978.
43. I. Kneppo Comparison Method of Measuring Q of Microwave Resonators, *IEEE Trans. Microw. Theory Tech.*, **MTT-25**: 423–426, 1977.
44. I. Kneppo Integration Method of Measuring Q of the Microwave Resonators, *IEEE Trans. Microw. Theory Tech.*, **MTT-26**: 131, 1978.
45. J. C. Liu *et al.* Accurate Measurement of the Q factor for the Cavity Perturbation Method, *Microw. Opt. Lett.*, **13**: 87–90, 1996.
46. R. K. Pandrangi S. S. Stuchly M. Barski A Digital System for Measurement of Resonant Frequency and Q Factor, *IEEE Trans. Instrum. Meas.*, **IM-31**: 18–21, 1982.
47. M. Linzer D. P. Stokesberry A Frequency Lock Method for the Measurement of Q Factors of Reflection and Transmission resonators, *IEEE Trans. Instrum. Meas.*, **IM-22**: 61–77, 1973.

48. G. Ghosh *et al.* Method of measuring loaded *Q*-factor of single ended cavity resonators using reflection bridge, *Rev. Sci. Instrum.*, **49** (3): 378–379, 1978.
49. M. C. Sanchez E. Martin J. M. Zamarro New Vectorial automatic technique for characterization of resonators, *IEE Proc.*, **136** (2): 147–150, 1989.
50. A. N. Luiten A. G. Mann D. G. Blair High Resolution measurement of the temperature-dependence of the *Q*, coupling and resonant frequency of a microwave resonator, *Meas. Sci. Tech.*, **7**: 949–953, 1996.
51. C. P. Hearn P. G. Bartley E. S. Bradshaw A modified *Q*-circle Measurement procedure for Greater Accuracy, *Microw. J.*, **36** (10): 108–111, 1993.
52. D. Kajfez Linear Fractional Curve Fitting for Measurement of High *Q* Factors, *IEEE Trans. Microw. Theory Tech.*, **MTT-42**: 1149–1153, 1994.
53. D. Kajfez *Q Factor*, Oxford, MS: Vector Forum, 1994.
54. E. Y. Sun S. H. Chao Unloaded *Q* measurement, *IEEE Trans. Microw. Theory Tech.*, **MTT-43**: 1983–1986, 1995.
55. D. Kajfez E. J. Hwan *Q*-Factor measurement with network analyzer, *IEEE Trans. Microw. Theory Tech.*, **MTT-32**: 666–670, 1984.
56. B. Sauer *et al.* Precise calibration of a microwave cavity with a non-ideal waveguide system, *Rev. Sci. Instrum.*, **62** (1): 189–197, 1991.
57. W. P. Wheless A resonator de-embedding procedure, *IEEE Trans. Microw. Theory Tech.*, **MTT-38**: 864–869, 1989.
58. D. Kajfez W. P. Wheless Invariant definitions of the unloaded *Q* factor, *IEEE Trans. Microw. Theory Tech.*, **MTT-34**: 840–841, 1986.
59. M. Fuchs Simple and accurate measurement of loaded *Q* factor of microwave oscillators using thermal noise injection, *Proc. 20th Eur. Microw. Conf.*, **1**: 512–516, 1990.
60. D. B. Leeson A simple model of feedback oscillator noise spectrum, *Proc. IEEE*, **54**: 329–330, 1966.
61. J. Krupka Computations of frequencies and intrinsic *Q* factors of TE_{0nm} modes of dielectric resonators, *IEEE Trans. Microw. Theory Tech.*, **MTT-33**: 1985.
62. C. Wang B. Q. Gao C. P. Deng Accurate study of *Q* factor of resonator by a finite difference time-domain method, *IEEE Trans. Microw. Theory Tech.*, **MTT-43**: 1524–1529, 1995.

ANDRE LUITEN
University of Western Australia